



Local structure and oxidation state of uranium in some ternary oxides: X-ray absorption analysis

A.V. Soldatov^{b,a,*}, D. Lamoen^a, M.J. Konstantinović^c, S. Van den Berghe^c,
A.C. Scheinost^{d,e}, M. Verwerft^c

^aTSM, Departement Fysica, Universiteit Antwerpen, Groenenborgerlaan 171, B-2020 Antwerpen, Belgium

^bFaculty of Physics, Rostov State University, Sorge 5, Rostov-on-Don, 344090, Russia

^cSCK-CEN, Reactor Materials Research, Boeretang 200, B-2400 Mol, Belgium

^dInstitute of Radiochemistry, Forschungszentrum Rossendorf e.V., P.O. Box 510119, D-01314 Dresden, Germany

^eRossendorf Beamline at ESRF, P.O. Box 220, F-38043 Grenoble, France

Received 3 May 2006; received in revised form 22 August 2006; accepted 24 August 2006

Abstract

We investigated the local atomic and electronic structures of two related systematic sets of ternary uranium oxides, NaUO_3 – KUO_3 – RbUO_3 and BaUO_3 – $\text{Ba}_2\text{U}_2\text{O}_7$ – BaUO_4 , by measuring the X-ray absorption near edge structure (XANES). The results are compared with calculations based on a self-consistent real space full multiple scattering analysis. We found a very good agreement between measured and calculated spectra, which indicates that the uranium ions are in a pure U^{5+} oxidation state in these compounds. The low energy shoulder observed in the U L_3 edge XANES is an intrinsic feature of the uranium unoccupied $6d$ electronic states of the U^{5+} ions within the studied materials. Specific double shoulder features in the higher energy range of the U L_3 edge XANES can be interpreted as indicative of the pure cubic perovskite structure.

© 2006 Elsevier Inc. All rights reserved.

Keywords: X-ray absorption fine structure; Local and electronic structure; Uranium oxides

1. Introduction

In spite of the large amount of chemical, crystallographic and thermodynamic data available, the knowledge of the rather complicated uranium ternary oxides is still far from complete. One of the key topics is the local structure around the uranium ions and consequently their exact oxidation state in various compounds [1]. Difficulties with assigning valences in uranium compounds have been reported [2] for KUO_3 , RbUO_3 , NaUO_3 . Formally, these structures contain only one uranium valence, namely U^{5+} . Their crystal structures are based on a perovskite structure with only one crystallographic position for U. As far as these two observations are concerned, there is no objection

against classifying these materials as pure monovalent compounds. However, it has been reported that the XPS spectra of these uranates exhibit doublet structures for the U4f peaks [2,3], which can be interpreted as a signature of a mixed valence state.

X-ray absorption fine structure (XAFS) spectroscopy is a well-recognized method to study the local environment of actinides in their compounds [4]. XAFS is divided into two regions: Extended X-ray absorption fine structure (EXAFS), and X-ray absorption near edge structure (XANES) [5]. The EXAFS data can be analyzed much easier, but contain only information on the radial distribution of atoms, while XANES analysis in principle allows one to define the full 3D local atomic geometry, including symmetry and fine details of the electronic structure of the materials under study. In order to extract the information from experimental X-ray absorption spectra, it is necessary to calculate these spectra using an advanced theoretical approach [6].

*Corresponding author. Faculty of Physics, Rostov State University, Sorge 5, Rostov-on-Don, 344090, Russia. Fax: +7 863 2975 120.

E-mail address: soldatov@phys.rsu.ru (A.V. Soldatov).

For about two decades, XAFS spectroscopy was successfully used for the investigations of uranium bearing materials [7–17], including micro-XANES methods [18,19] and the study of oxygen XANES in uranium oxides [20,21]. Until now, the uranium XANES was mostly used without detailed theoretical analysis, as an empirical “finger-print” approach to study the most probable local structure around uranium ions (“uranyl” or “uranate” classification), or chemical shift analysis for the investigation of the uranium oxidation state.

In the present study the U L_3 edge XANES spectra have been measured in KUO_3 , RbUO_3 , NaUO_3 , BaUO_3 , $\text{Ba}_2\text{U}_2\text{O}_7$ and BaUO_4 and theoretical self-consistent field (SCF) full multiple scattering (FMS) simulations of XANES spectra have been performed for the analysis of the local atomic and electronic structure in these materials.

2. Experiment and computational method

The sample preparation method used for synthesizing the AUO_3 powders with $A = \text{Na, K, Rb}$ is described elsewhere [22]. For the barium compounds, similar methods were used. Stoichiometric quantities of the starting materials, barium carbonate BaCO_3 and uranium oxide U_3O_8 were intimately mixed using a mortar and pestle. For BaUO_4 , this mixture was treated in a box furnace at 900 °C in air. BaUO_4 was reduced to BaUO_3 at 1400 °C in a flow of dried $\text{Ar}/5\%\text{H}_2$ (dew point < −50 °C). The preparation of $\text{Ba}_2\text{U}_2\text{O}_7$, starting from BaUO_4 , requires accurate oxygen potential control, since this compound is only stable in a restricted oxygen potential domain [23]. This control can be achieved by mixing $\text{Ar}/5\%\text{H}_2$ gas with $\text{Ar}/5000\text{ ppm O}_2$ gas in the appropriate quantities to establish the correct μ_{O_2} of −330 kJ/mol in the furnace at the treatment temperature of 1000 °C.

For the XAS measurements, a small quantity of each uranate (about 20 mg) was intimately mixed with boron nitride (BN), pressed into pellets and loaded in sealed, X-ray transparent containers. Uranium L_3 -edge X-ray absorption spectra were collected at the Rossendorf Beamline (ROBL) at bending-magnet port BM 20, of the European Synchrotron Radiation Facility (ESRF) in Grenoble. The monochromator equipped with Si(111) double-crystal was used in channel-cut mode. Higher harmonics were rejected by two Pt-coated mirrors. The first mirror collimates the X-ray beam onto the monochromator crystal, the second mirror focuses the beam vertically to the sample. The vertical width of the secondary slit was 1.0 mm. Uranium L_{III} -edge spectra were collected in transmission mode using argon-filled ionization chambers at ambient temperature and pressure. Data was collected in equidistant energy steps of 1.0 eV across the XANES region. Note that the energy resolution of the Si(111) crystal is about 3.5 eV at the U L_3 -edge. An Y metal foil (first inflection point at 17038 eV) was used for energy calibration.

Theoretical analysis of the U L_3 edges, was carried out on the basis of a SCF FMS method as it is implemented in FEFF8.4 code. The importance of the SCF approach to obtain a reasonable crystal potential for plutonium oxides and hydrides in XANES analysis has been shown before [24,25]. The algorithm for the FMS method has been described elsewhere [26]. Phase shifts of the photoelectron were calculated in the framework of the self-consistent crystal muffin-tin (MT) potential scheme with 15% overlapping MT spheres. The spectra have been simulated using several types of exchange potentials: non-local potential, Dirac-Fock potential, Hedin-Lundqvist potential and Dirac-Hara potential. Dependence of spectra on a relaxation of electrons in the presence of a core-hole has been studied as well. The best agreement with experiment has been achieved for the spectra calculated with the Hedin-Lundqvist potential in the presence of a core-hole. For the experimental energy resolution, a value of 2.0 eV was used. These factors were treated as contributions to the imaginary part of the self-energy term. Self-consistent potentials and corresponding phase-shifts were calculated for clusters of atoms having 5.0 Å radii, while FMS calculations of the U L_3 XANES were performed for atomic clusters of 8.0 Å radii.

For XANES spectra simulations, we have used the following crystallographic data: KUO_3 — $Pm\bar{3}m$ (#221 space group) perfect perovskite structure with lattice parameter $a = b = c = 4.293$ Å [22]; RbUO_3 — $Pm\bar{3}m$ (#221 space group) perfect perovskite structure with lattice parameter $a = b = c = 4.322$ Å [22]; NaUO_3 — $Pbnm$ (#62 space group) orthorhombic structure with lattice parameters $a = 5.7739$ Å, $b = 5.9051$ Å, $c = 8.2784$ Å [22]; BaUO_4 — $Pbcm$ (#57 space group) orthorhombic structure with lattice parameters $a = 5.744$ Å, $b = 8.136$ Å, $c = 8.237$ Å [27]. For BaUO_3 two possible structures have been tested, namely the ideal cubic perovskite group #221($Pm\bar{3}m$) with $a = b = c = 4.4074$ Å [28], and the orthorhombic $Pnma$ (#62 space group) structure with the following lattice parameters $a = 6.2094$ Å, $b = 8.7987$ Å, $c = 6.2370$ Å [29]. For $\text{Ba}_2\text{U}_2\text{O}_7$, the crystal structure reported in [23] was considered incorrect because of an unphysical O–O distance. The structure of this compound was refined on the basis of new X-ray diffraction data and the resulting structure was described in space group $Imma$ (#74 space group) with $a = 8.161$ Å, $b = 11.317$ Å, $c = 8.185$ Å [S. Van den Bergh, to be published].

3. Results and discussion

In Fig. 1a, comparison between experimental and theoretical U L_3 edge XANES of KUO_3 and RbUO_3 crystals is presented. Since these materials have very similar crystal lattices and the same oxidation state of the uranium ions (U^{5+}), the XANES spectra look very similar: the lowest energy structure is the peak A with a low energy shoulder A_1 which is found to be a characteristic feature for all U^{5+} compounds in the present study. In the higher

energy region of the XANES, we observed the shoulders B and C, which in our interpretation originate from the perfect perovskite structure (#221 space group) of the ternary uranium. From the relative energy shift of the C shoulder, it is easy to conclude that the U–O interatomic distances must be larger in RbUO₃ than in KUO₃. According to Natoli's rule [5], $R^2 \cdot \Delta E = \text{constant}$, where

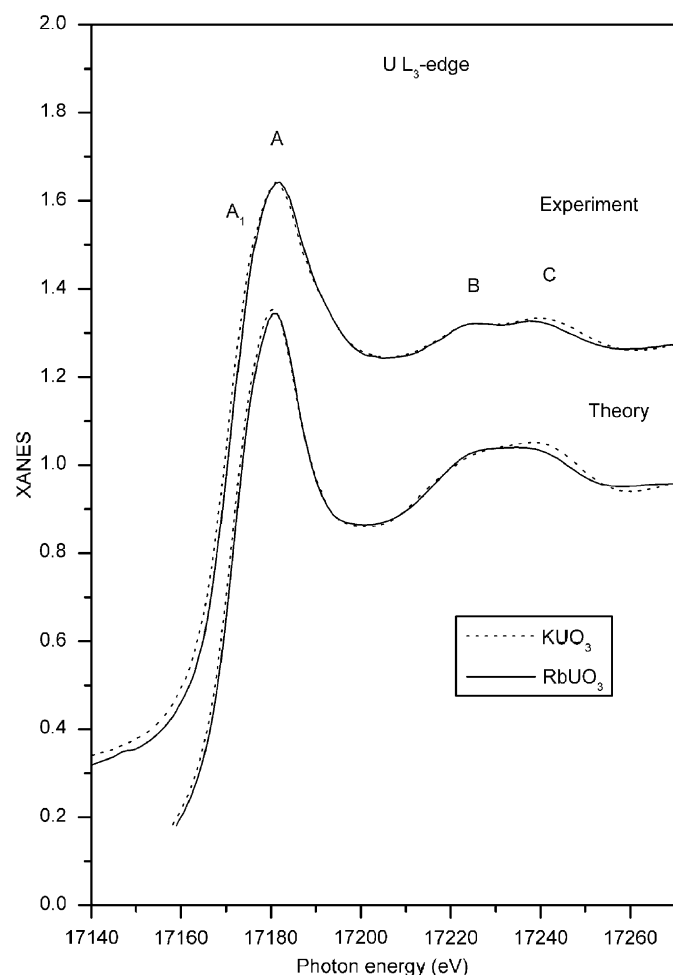


Fig. 1. Comparison of the experimental U *L*₃ edge XANES in KUO₃ and RbUO₃ with the theoretical spectra.

R are the interatomic distances between nearest neighbors and ΔE is the energy separation between characteristic peaks of XANES. This rule applies well for uranyl ions complexed with organic acids [30]. Analysis of the U–O interatomic distances for KUO₃ and RbUO₃ is presented in Table 1 and indicates that the XANES method is sensitive enough to probe changes in the interatomic distances as small as 0.02 Å. Fig. 1 also demonstrates that the present SCF FMS approach reproduces all features of the U *L*₃ edge XANES in both KUO₃ and RbUO₃, including small energy shifts of the C peak, and the changes in the peak intensities. Thus, the theoretical framework was found to be quite adequate for detailed analysis of the U *L*₃ edge XANES in ternary uranium oxides.

As one can see in Fig. 2, where we present a comparison between the experimental and theoretical U *L*₃ edge XANES spectra of KUO₃ and NaUO₃, all changes can be reproduced by our theoretical model. We already mentioned that substitution of potassium by sodium in an AUO₃ crystal results in the distortion of the lattice with a corresponding transition from the perfect perovskite structure (#221 space group for KUO₃) to the orthorhombic structure (#62 space group for NaUO₃). One can find in Fig. 2 a clear evidence that the double B–C shoulder at the high energy region of the XANES spectrum (see Fig. 1), which is characteristic for the perfect cubic perovskite lattice of KUO₃ (as well as for RbUO₃), merged into a single shoulder B₁ at about 17,230 eV for the orthorhombic NaUO₃. Thus, one can use these “finger-print” shoulders in the high energy region of the U *L*₃ edge XANES to get an idea about the magnitude of the local distortions from the cubic symmetry in these ternary uranium oxides. At the same time, the main white lines for all three U⁵⁺ materials studied above (KUO₃, RbUO₃ and NaUO₃) have the same asymmetric structure with a low energy shoulder A₁. For the materials studied in the present work an analysis of the U d DOS calculated within *L*₃ core-hole potential shows that the low energy shoulder in U *L*₃-edge XANES is found to be a specific feature for U⁵⁺ compounds, but the absence of this shoulder on the U *L*₃ edge of BaUO₄ can be accidental and not specific for other U⁶⁺ oxides.

Table 1

Parameters of local structure around uranium ions and their states in the compounds under the study

Compound	U oxidation	Symmetry group number	Number of O atoms around U	U–O distances used for simulations (Å)
KaUO ₃	U ⁵⁺	221	6	2.146
RbUO ₃	U ⁵⁺	221	6	2.161
NaUO ₃	U ⁵⁺	62	2	2.142
			4	2.151
BaUO ₃	U ⁴⁺	62	2	2.191
			4	2.235–2.246
BaUO ₄	U ⁶⁺	57	2	1.87
			4	2.19–2.22
Ba ₂ U ₂ O ₇	U ⁵⁺	74	4 (U ₁)	2.177
			2 (U ₁)	2.183
			2 (U ₂)	1.968
			4 (U ₂)	2.156

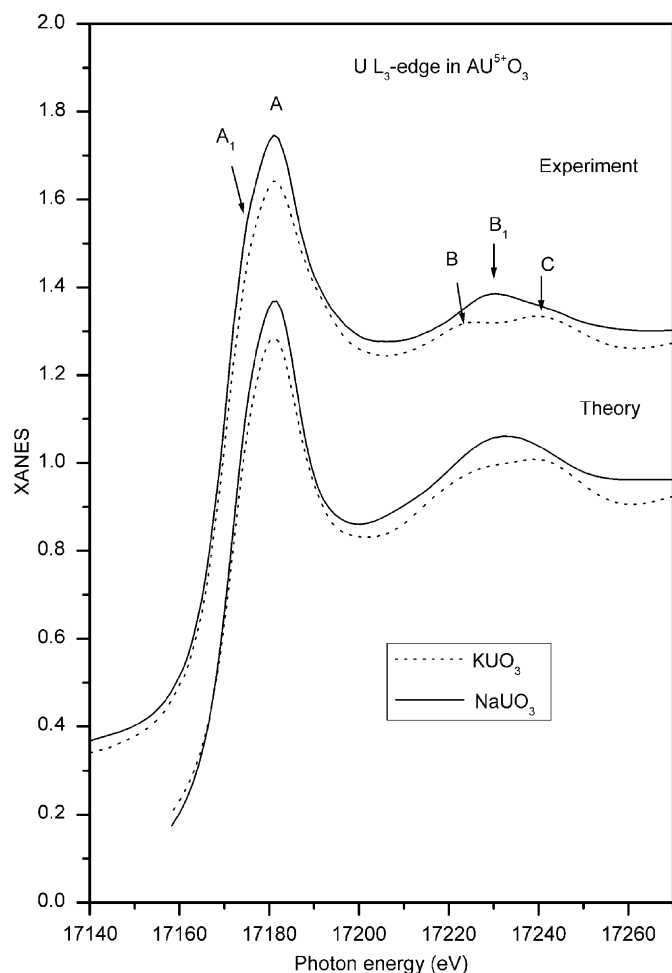


Fig. 2. Comparison of the experimental U L_3 edge XANES in KUO_3 and $NaUO_3$ with the theoretical spectra.

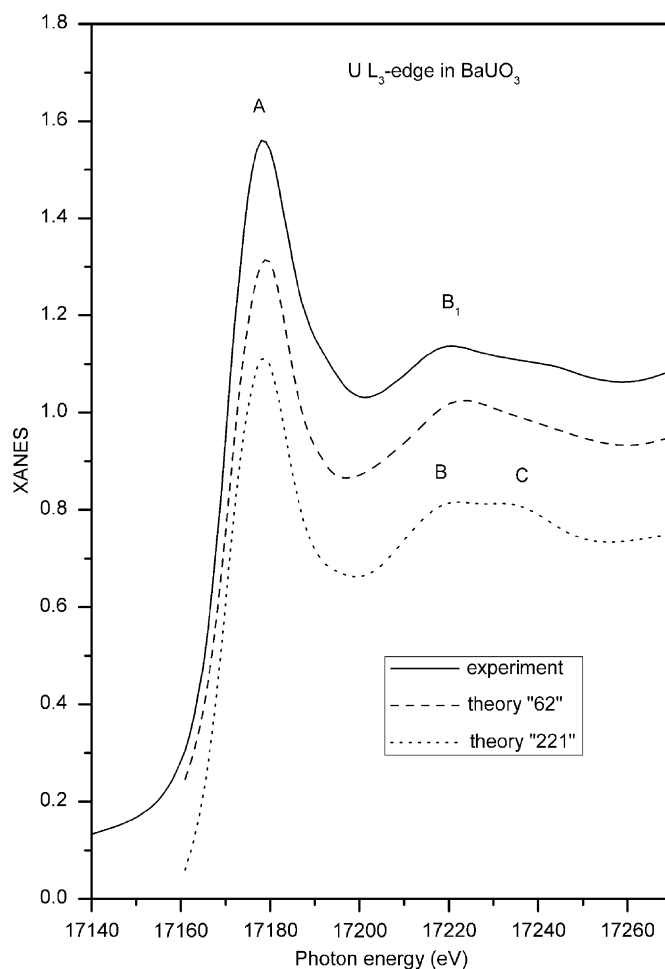


Fig. 3. Comparison of the experimental U L_3 edge XANES in $BaUO_3$ with the theoretical spectra. Calculated for two possible structural models (see text).

Let us now consider $BaUO_3$. This compound is known to readily deviate from stoichiometry and as such, different structures have been reported. In [29], a compound with $Ba_{0.98}UO_3$ stoichiometry has been described in the orthorhombic space group #62. Later, a perfect cubic perovskite structure has been proposed for $BaUO_{3.023}$ [28], but it was finally reported that the attempts to prepare fully stoichiometric $BaUO_3$ were not successful and that the obtained material ($BaUO_{3.05}$) must be refined as having the orthorhombic #62 symmetry group [31]. For the powder prepared in the framework of this study, a slight over-stoichiometry can be expected due to oxidation in air. Thus, we performed the simulation of the U L_3 edge XANES for $BaUO_3$ assuming two possible crystal lattice symmetries. In Fig. 3 we show a comparison between the experimental U L_3 edge XANES in $BaUO_3$ and theoretical spectra calculated for both cubic (#221 space group) and orthorhombic (#62 space group) crystal lattices. As one can see, the experimental spectrum agrees better with the theoretical one obtained by assuming the orthorhombic symmetry. Therefore, the $BaUO_3$ sample used in the present study has, most likely, orthorhombic symmetry (group #62). This was confirmed by subsequent electron

diffraction experiments in a Transmission Electron Microscope, where the deviation from cubic symmetry was clearly established. It is anticipated that tilting of the UO_6 octahedra occurs, and for symmetry $Pnma$, the expected tilting scheme is $(a-b+a-)$. This results in unit cell dimensions of $\sqrt{2}a \times 2a \times \sqrt{2}a$ with a the pseudocubic unit cell parameter. Although deviation from cubic symmetry was clearly evidenced, the electron diffraction experiments failed to identify unit cell multiplication and a tilting scheme could not be determined. A further study by neutron diffraction might enable the determination of the tilting scheme by refining the oxygen atom positions which are mostly affected by the expected tilting of the UO_6 octahedra.

$Ba_2U_2O_7$ has a structure which is more complex than the cubic perovskites, with two inequivalent positions of uranium ions (one can see nearest neighborhood around these two sites in Fig. 4). We refer to these two positions as U_1 and U_2 in Fig. 5 and in the following discussion. In Fig. 5, we present a comparison of the experimental U L_3 edge XANES in $Ba_2U_2O_7$ with the theoretical spectra calculated for two structural models. Initially we have

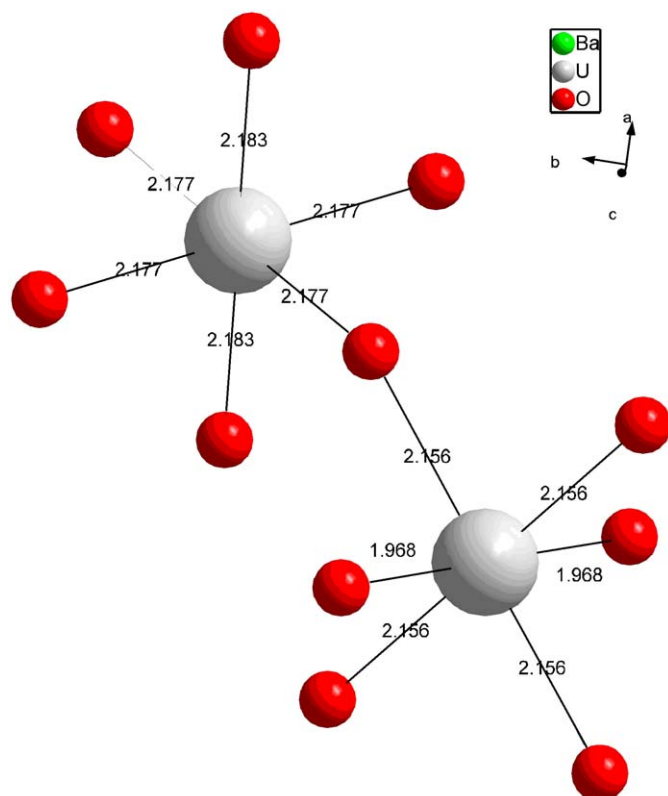


Fig. 4. Local structure around two nonequivalent uranium sites in $\text{Ba}_2\text{U}_2\text{O}_7$.

considered the structure published in Ref. [23], but the shape of the theoretical XANES have been found to differ significantly from the experimental data. As one can see in Fig. 4 the shapes of XANES calculated for both U_1 and U_2 types of uranium atoms differ from the experimental spectrum, as well as the total theoretical spectrum. Therefore, we have performed a refinement based on the X-ray diffraction data for $\text{Ba}_2\text{U}_2\text{O}_7$ (see Table 2). Although neutron diffraction data are required for a more accurately study of the positions of the oxygen atoms, the new refinement provides very satisfying results. Although the refinement was performed unbiased, the uranium local environments are now very similar (as can also be seen from the theoretical calculations of the XANES components). With these new structural parameters, the theoretical XANES spectrum at the U L_3 edge agrees well with the experimental data. Small variations in the environments of the U_1 and U_2 ions (one can find numerical parameters in Table 1) result in variations of the partial XANES shapes, showing the sensitivity of XANES spectroscopy to small changes in local structure around the specific atomic site and also increasing the confidence in the correctness of the refined structure.

To study the effect of changes in the uranium oxidation state on the shape of U L_3 edge XANES, we present in Fig. 6 a comparison of the experimental and theoretical U L_3 edge XANES in two isostructural materials— $\text{BaU}^{4+}\text{O}_3$, $\text{NaU}^{5+}\text{O}_3$ that have uranium ions in different

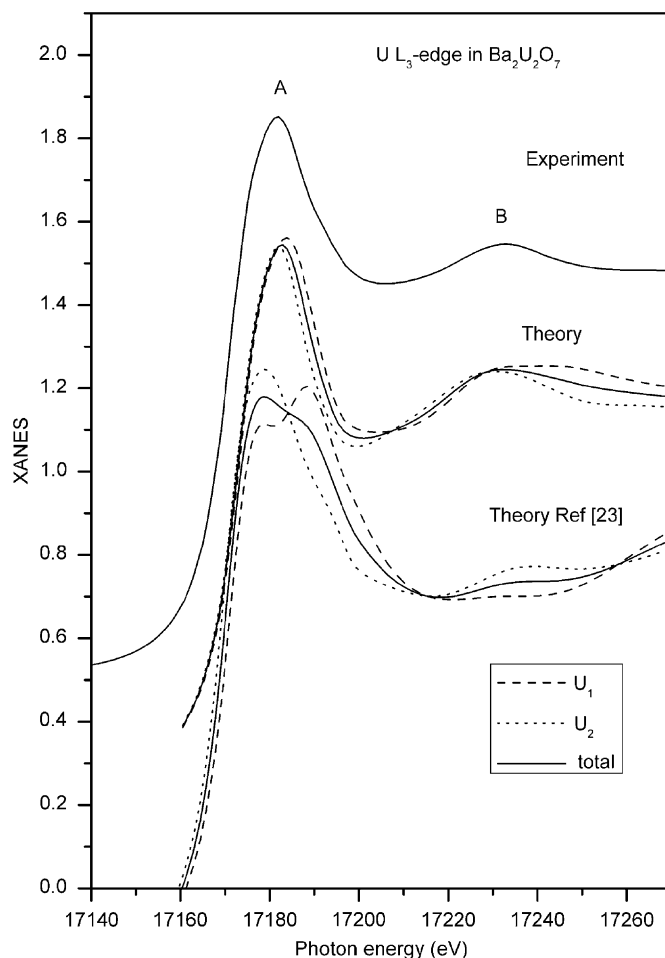


Fig. 5. Comparison of the experimental U L_3 edge XANES in $\text{Ba}_2\text{U}_2\text{O}_7$ with the theoretical spectra.

Table 2

Results of the refinement of the $\text{Ba}_2\text{U}_2\text{O}_7$ structure based solely on the X-ray diffraction data

Element	Wyck	x	y	z
Ba1	4a	0	0	0
Ba2	4d	$\frac{1}{4}$	$\frac{1}{4}$	$\frac{3}{4}$
U1	4c	$\frac{1}{4}$	$\frac{1}{4}$	$\frac{1}{4}$
U2	4b	0	0	$\frac{1}{2}$
O1	4e	0	$\frac{1}{4}$	0.155(3)
O2	8h	0	0.592(2)	0.296(2)
O3	16j	0.302(2)	0.117(1)	0.065(2)

oxidation states. It must be stressed that, in order to get a clear understanding of the influence of the oxidation state of the ion, one preferably needs to analyze the XANES of isostructural materials, or materials with very similar crystal structures. Accordingly, we used NaUO_3 , rather than $\text{Ba}_2\text{U}_2\text{O}_7$ for this comparison. Alternatively, the modifications of the XANES shape that originate from the differences in the crystal symmetries can affect significantly the energy position of the inflection point of

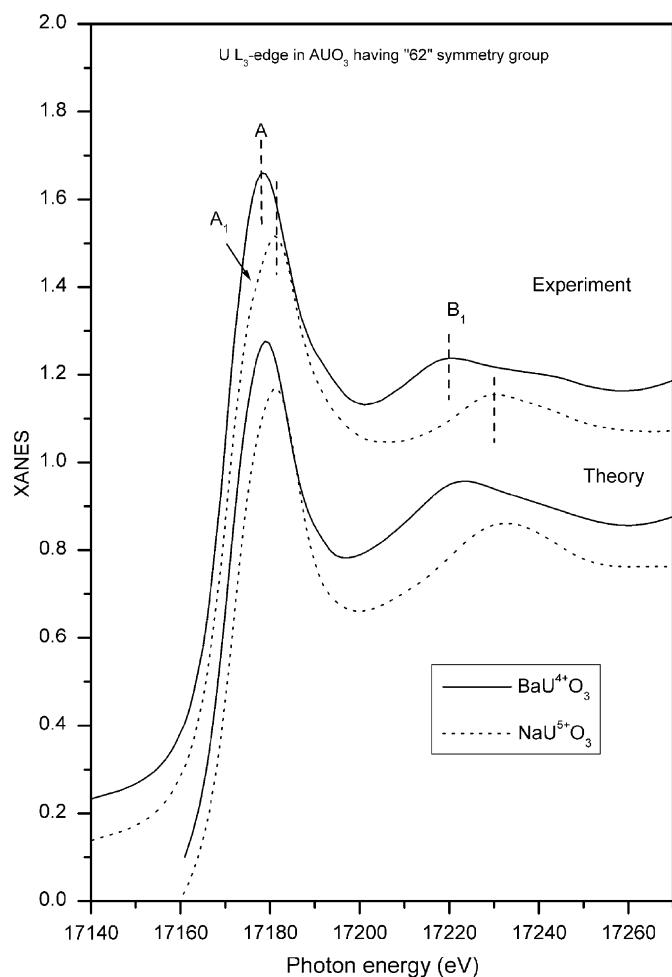


Fig. 6. Comparison of the experimental U L_3 edge XANES in BaUO_3 and NaUO_3 with the theoretical spectra.

the main rising edge of XANES (this point is generally used in the study of the chemical shifts in XANES analysis). As one can see in Fig. 6, when the oxidation state of the uranium ion changes from U^{5+} (NaUO_3) to U^{4+} (BaUO_3), the shape of the main white line of the U L_3 edge changes significantly (namely the low energy shoulder A_1 disappears and the white line becomes a symmetric one). On the other hand, the high-energy shoulder B_1 has the same shape for both materials, but is significantly shifted to higher energies in the case of NaUO_3 . Using the semi-empirical rule mentioned above one can conclude that the U–O distance must be much smaller in NaUO_3 than in BaUO_3 , which is in agreement with experiment (see Table 1). As in all previous cases we find a very good agreement between experimental and theoretical XANES for BaUO_3 .

To study the applicability of the chemical shift analysis for the determination of the oxidation state of uranium ion in ternary oxides, we have compared in Fig. 7 the renormalized (to have the same intensity as the main peak A) experimental U L_3 edge XANES in BaUO_3 , NaUO_3 and $\text{Ba}_2\text{U}_2\text{O}_7$. It is observed that the tailing of the low energy shoulder A_1 in the $\text{NaU}^{5+}\text{O}_3$ results in shifting of the inflection point of its rising edge so significantly, that,

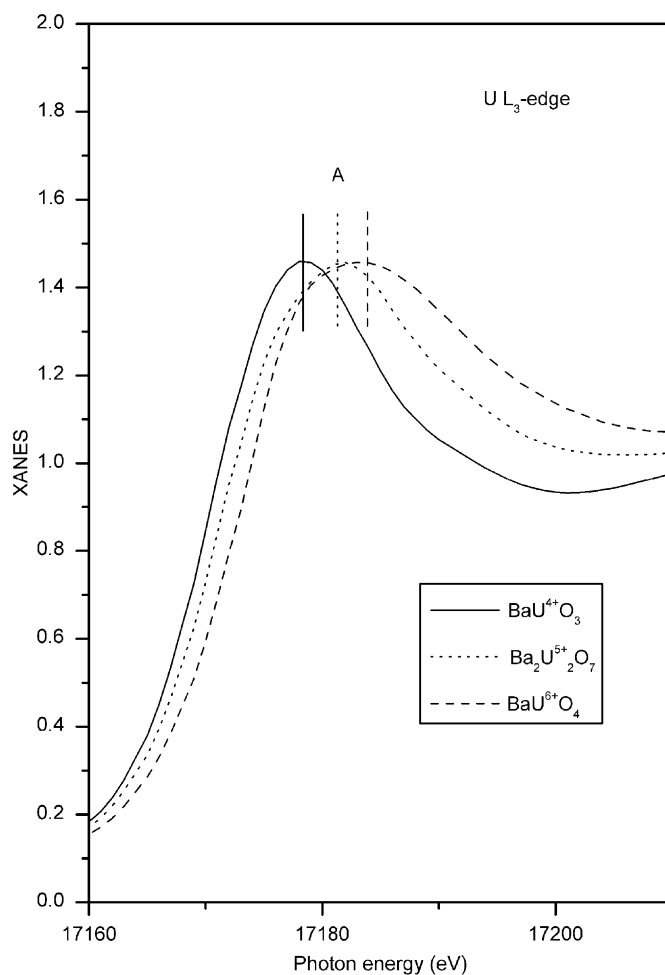


Fig. 7. Comparison of the renormalized (see text) experimental U L_3 edge XANES in BaUO_3 , $\text{Ba}_2\text{U}_2\text{O}_7$ and BaUO_4 .

for this case, one cannot use the standard method to analyze the oxidation state. Thus, in the present case it will be better to use the position of the main maximum A as a control point for the determination of the uranium ion oxidation state.

To show that the SCF FMS method reproduces well enough the XANES data for ternary uranium oxides having different oxidation states of uranium, we present in Fig. 8 a comparison of the experimental U L_3 edge XANES in BaUO_3 , $\text{Ba}_2\text{U}_2\text{O}_7$ and BaUO_4 (normalized) with the corresponding theoretical spectra.

By analysis of the shape of the main white line, one can conclude that the asymmetry of the main white line of the U^{5+} ions in ternary oxides is a characteristic feature of this oxidation state that does not depend on the crystal structure. When the oxidation state changes to U^{4+} or U^{6+} , the symmetry of the main peak of the white line is restored. Thus, in this respect, the XANES calculations and data do not support the assumption of mixed valence in these compounds.

In view of the previously observed X-ray dichroism near the U L_3 edge in rubidium uranyl nitrate [32], it would be interesting for future work to measure and analyze

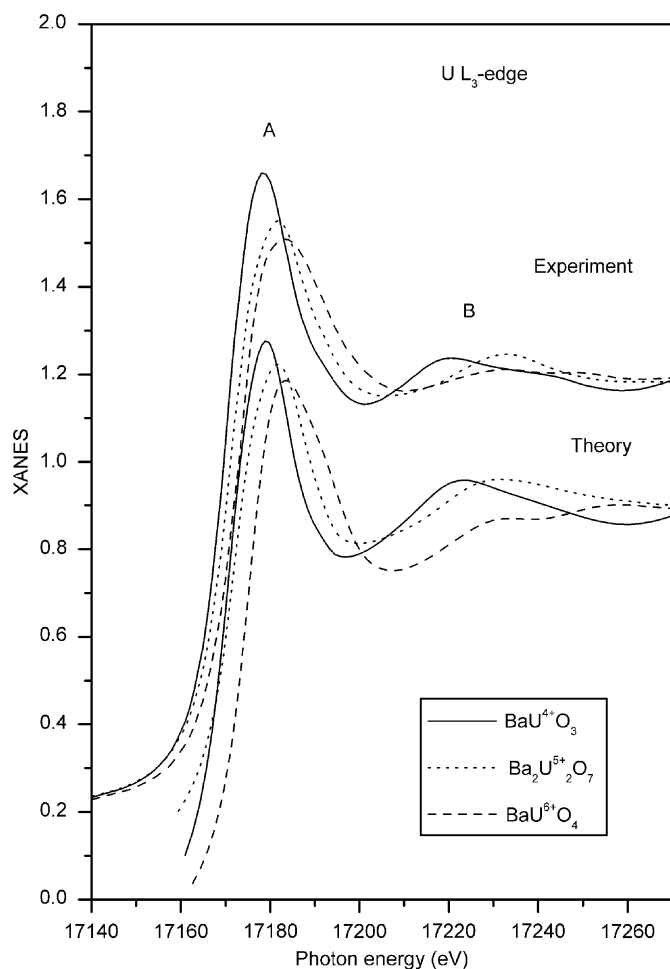


Fig. 8. Comparison of the experimental U L_3 edge XANES in BaUO_3 , BaUO_4 and $\text{Ba}_2\text{U}_2\text{O}_7$ with the theoretical spectra.

theoretically the polarized U L_3 -edge in the compounds under study to obtain more specific information on the electronic structure of these materials.

4. Conclusions

The SCF FMS method was found to be an adequate tool for the analysis of the U L_3 -edge XANES of ternary uranium oxides. The calculated XANES spectra of the investigated compounds correspond very well with the experimental results and reproduce all features related to the valence changes between BaUO_4 , $\text{Ba}_2\text{U}_2\text{O}_7$ and BaUO_3 , as well as the variation in crystal structure between the cubic perovskite KUO_3 and RbUO_3 and the distorted, orthorhombic NaUO_3 . It could be concluded that the XANES theoretical and experimental results support the assumption that only U^{5+} ions are present in NaUO_3 , KUO_3 and RbUO_3 , as well as in $\text{Ba}_2\text{U}_2\text{O}_7$.

Acknowledgments

A.V. Soldatov gratefully acknowledges financial support from the Bijzonder Onderzoeksfonds (BOF) of the Uni-

versiteit Antwerpen. The study was performed in the framework of the European Network of Excellence “ACTINET”.

References

- [1] L.R. Morss, N.M. Edelstein, J. Fuger, J.J. Katz (Eds.), *The Chemistry of the Actinide and Transactinide Elements*, Springer, Berlin, 2006 3015pp.
- [2] S. Van den Berghe, M. Verwerft, J.-P. Laval, B. Gaudreau, P.G. Allen, A. Van Wyngarden, *J. Solid State Chem.* 166 (2002) 320–329.
- [3] G.C. Allen, J.A. Crofts, M.T. Curtis, P.M. Tucker, *J. Chem. Soc. Dalton Trans.* (1974) 1296–1301.
- [4] M.A. Denecke, *Coord. Chem. Rev.* 250 (2006) 730–754.
- [5] A. Bianconi, in: R. Prins, D.C. Koningsberger (Eds.), *X-ray Absorption: Principles, Applications and Techniques of EXAFS, SEXAFS and XANES*, Wiley, New York, 1988, p. 573.
- [6] G. Smolentsev, A.V. Soldatov, *J. Synchrotron Radiat.* 13 (2006) 19–29.
- [7] J. Petiau, G. Calas, D. Petitmaire, A. Bianconi, M. Benfatto, A. Marcelli, *Phys. Rev. B* 34 (1986) 7350–7361.
- [8] G. Kalkowski, G. Kaindl, W.D. Brewer, W. Krone, *Phys. Rev. B* 35 (1987) 2667–2677.
- [9] S. Van den Berghe, M. Verwerft, J.-P. Laval, B. Gaudreau, P.G. Allen, A. Van Wyngarden, *J. Solid State Chem.* 166 (2002) 320–329.
- [10] C. Den Auwer, E. Simoni, S. Conradson, C. Madic, *Eur. J. Inorg. Chem.* (2003) 3843–3859.
- [11] E.M. Pierce, J.P. Icenhower, R.J. Serne, J.G. Catalano, *J. Nucl. Mater.* 345 (2005) 206–218.
- [12] A. Bombardi, F. d’Acapito, K. Mattenberger, O. Vogt, G.H. Lande, *Phys. Rev. B* 68 (2003) 104414.
- [13] J.G. Lack, S.K. Chaudhuri, S.D. Kelly, K.M. Kemner, S.M. O’Connor, J.D. Coates, *Appl. Environm. Microbiol.* 68 (2002) 2704–2710.
- [14] T. Allard, P. Ildenfonse, C. Beaucaire, G. Calas, *Chem. Geol.* 158 (1999) 81–103.
- [15] S.D. Conradson, B.D. Begg, D.L. Clark, C. den Auwer, M. Ding, P.K. Dorhout, F.J. Espinosa-Faller, P.L. Gordon, R.G. Haire, N.J. Hess, R.F. Hess, D. Webster Keogh, G.H. Lander, D. Manara, L.A. Morales, M.P. Neu, P. Paviet-Hartmann, J. Rebizant, V.V. Rondinella, W. Runde, C. Drew Tait, D. Kirk Veirs, P.M. Villella, F. Wastin, *J. Solid State Chem.* 178 (2005) 521–535.
- [16] F. Farges, C.W. Ponander, G. Calas, G.E. Broun Jr., *Geochim. Cosmochim. Acta* 56 (1992) 4205–4220.
- [17] J.A. Fortner, A.J. Kropf, R.J. Finch, A.J. Bakel, M.C. Hash, D.B. Chamberlain, *J. Nucl. Mater.* 304 (2002) 56–62.
- [18] S. Torok, J. Osan, L. Vincze, S. Kurunczi, G. Tamborini, M. Betti, *Spectrochim. Acta B* 59 (2004) 689–699.
- [19] B. Salbu, K. Janssens, O.C. Linda, K. Proost, L. Gijssels, P.R. Danesi, *J. Env. Radioact.* 78 (2005) 125–135.
- [20] F. Jollet, T. Petit, S. Gota, N. Thromat, M. Gautier-Soyer, A. Pasturel, *J. Phys.: Condens. Matter* 9 (1997) 9393–9401.
- [21] G.E. Yalovega, A.V. Soldatov, *Phys. Solid State* 41 (1999) 1268–1270.
- [22] E.H.P. Cordfunke, D.J.W. Ijdo, *J. Phys. Chem. Solids* 49 (5) (1988) 551–554.
- [23] A.L. Ankudinov, B. Ravel, J.J. Rehr, S.D. Conradson, *Phys. Rev. B* 58 (1998) 7565–7576.
- [24] A.L. Ankudinov, S.D. Conradson, J. Mustre de Leon, J.J. Rehr, *Phys. Rev. B* 57 (1998) 7518–7525.
- [25] J.J. Rehr, A.L. Ankudinov, *Coord. Chem. Rev.* 249 (2005) 131–140.
- [26] S. Van den Berghe, A. Leenaers, C. Ritter, *J. Solid State Chem.* 177 (2004) 2231–2235.
- [27] A.H. Reis Jr., H.R. Hoekstra, E. Gebert, S.W. Peterson, *J. Inorg. Nucl. Chem.* 38 (1976) 1481–1485.
- [28] Y. Hinatsu, *J. Solid State Chem.* 102 (1993) 566–569.

- [29] S.A. Barrett, A.J. Jacobson, B.C. Tofield, B.E.F. Fender, *Acta Cryst. B* 38 (1982) 2775–2781.
- [30] M.A. Denecke, T. Reich, M. Bubner, S. Pompe, K.H. Heise, H. Nitsche, P.G. Allen, J.J. Bucher, N.M. Edelstein, D.K. Shuh, *J. Alloys Compd.* 271–273 (1998) 123–127.
- [31] E.H.P. Cordfunke, A.S. Booiij, V. Smit-Groen, P. van Vlaanderen, *J. Solid State Chem.* 131 (1997) 341–349.
- [32] D.H. Templeton, L.K. Templeton, *Acta Cryst. A* 38 (1982) 62–67.